PV and EV Capabilities for Improving Technical Conditions in Active Distribution Network

Marina Dubravac[1], Danijel Topić[1], Krešimir Fekete[1], Edin Lakić[2]
[1]*J. J. Strossmayer University of Osijek, Faculty of Electrical Engineering, Computer Science and Information Technology Osijek, Osijek, Croatia*
marina.dubravac@ferit.hr, danijel.topic@ferit.hr, kresimir.fekete@ferit.hr
[2]*Institute for Innovation and Development of University of Ljubljana, Ljubljana, Slovenia*
edin.lakic@iri.uni-lj.si

***Abstract*—Today many end-users have installed photovoltaic (PV) systems on their rooftops and exceedingly own electric vehicles (EVs). Integrating PV systems and EVs can harm technical conditions in distribution networks (DNs). Since both are inverter-based sources they have the capability of active power curtailment (APC) and reactive power control (RPC) and can provide ancillary service to the distribution system operator (DSO). In line with that, this paper proposes an optimal power flow (OPF) based model to improve technical conditions considering the capabilities of PV and EV inverters. The optimization problem is defined as nonlinear programming (NLP) due to full AC power flows and is solved with a co-simulation optimization approach. The effectiveness of the proposed model is tested through several case studies over low-voltage DN created according to real-life examples. Preliminary results suggest the significant importance of ancillary services provided by PV and EV inverters for improving DN operation.**

***Index Terms*—Active distribution network, Ancillary services, Co-simulation optimization approach, PV and EV inverter capabilities, Optimal power flow**

I. Introduction

European energy policies have been increasingly adopted toward renewable energy resources (RES), especially in response to climate change. As a result, previous passive consumers have become active consumers or prosumers through high integration of photovoltaic (PV) systems, energy storage systems (ESS), and exceedingly owning controllable loads such as electric vehicles (EVs). High integration of PV systems and EVs can harm technical conditions in distribution networks (DNs). Since both have an inverter in their configuration and have the capability of volt-watt control known as active power curtailment (APC) and volt-var control known as reactive power control (RPC), they can provide ancillary service and participate in the mitigation of their negative impact to DN [1]–[3].

Authors in literature [4] deal with EV charging management in PV-rich DN for reducing the cost of APC. First, the maximum power injection in each node is calculated and obtained according to voltage sensitivity. After that different scenarios of EV charging management are conducted: unmanaged, managed and (vehicle-to-grid) V2G concept. According to the obtained results, EV charging management successfully reduces PV APC and ensures energy and cost savings for PV owners. The aim of [5] is to reduce voltage violations and voltage unbalance as well as maximize PV hosting capacity in observed DN. The optimization model consists of two stages: day-ahead EV charging scheduling and real-time dynamic local control for providing ancillary services. Results show the effectiveness of the proposed model in providing network operation support. Paper [6] presents the optimal strategy for EV and PV placement and voltage regulators in order to enhance PV and EV hosting capacity in unbalanced DN. Obtained results show that the optimal location of voltage regulators, PV and EV and voltage control improve PV and EV hosting capacity. Authors in [7] propose EV charging and discharging pattern algorithm for voltage violation mitigation in DN without any voltage regulation. The algorithm includes both active and reactive power injections into the DN. Obtained results show that EV charging and discharging patterns have the potential to provide ancillary services to DSO. Authors in literature [8] propose an OPF-based model for controlling PV inverter capabilities and EV charging and discharging patterns to minimize operation cost and voltage violation in DN. The paper shows the potential of PVs and EVs to enhance power quality in DN. The OPF-based model for minimizing power exchange between upper and observed DN using the V2G concept is presented in [9]. First, the optimal location of EV chargers is obtained. After that, the proposed model is evaluated under different scenarios that consider optimal EV charging and discharging patterns. According to the obtained results, the proposed model not only reduces power exchange but also improves voltage stability and load profiles.

As an extension of the previous paper [10] in which authors proposed an OPF-based model for improving technical conditions using only the capabilities of PV inverters, this paper introduces the capabilities of EV inverters for providing ancillary services to DSO. The EV charging profile is obtained using an optimization-based approach and real-life measurement. The optimization-based approach gives EV charging profile according to day-ahead prices. The first step in this paper is to study the impact of PVs and EVs on energy losses and voltages in residential DN. After that, different PV inverter - APC and RPC capabilities and their combination with EV inverter capability similar to PV APC are tested. The

979-8-3315-1278-1/25/$31.00

problem is defined as nonlinear programming (NLP) due to full AC power flow without transformation. For this reason, the co-simulation optimization approach is used to obtain a feasible solution. The OPF-based model is evaluated on publicly available low-voltage DN.

The paper is organized as follows: mathematical formulation of optimization-based EV charging profile and OPF-based model with included objective function, network constraints and decision variable bounds are presented in Section 2. Section 3 introduces the proposed optimization framework, briefly describes test network model and presents case studies. The obtained results with discussion are presented in Section 4. The last section, Section 5, gives the conclusion of the paper.

II. Methodology

This section presents the mathematical formulation for an optimization-based EV charging profile. After that, the OPF-based model is formulated and described.

A. The mathematical formulation for a model of optimization-based EV charging profile

The optimization-based model for the EV charging profile is obtained according to day-ahead prices. The problem is coded in opened source *Python*-based optimization modeling language *Pyomo*. The optimization model is defined as linear programming (LP) and solved with IPOPT. The objective function refers to minimizing the cost of charging and it is described in (1).

$$min \sum_{t=1}^{T} c_t \cdot P_{ch,t} \tag{1}$$

where c_t presents day-ahead electricity prices scaled to €/kWh from [11] and $P_{ch,t}$ presents EV charging power.

Battery state of charge (SoC) for the first point of time is given in (2).

$$SoC_t = SoC_{initial} + P_{ch,t} \cdot \eta \tag{2}$$

where:

$P_{ch,t}$ – EV charging power,

η – charging efficiency.

SoC for each subsequent point of time is presented in (3).

$$SoC_t = SoC_{t-1} + P_{ch,t} \cdot \eta \tag{3}$$

SoC for the last point of time is presented in (4).

$$SoC_t = SoC_{last} + P_{ch,t} \cdot \eta \tag{4}$$

The first decision variable bound includes maximum EV charging power P_{ch}^{max} (5).

$$0 \leq P_{ch,t} \leq P_{ch}^{max} \tag{5}$$

The second decision variable defines the desired SoC (SoC^{max}) by EV owner (100%) in (6).

$$0 \leq SoC_t \leq SoC^{max} \tag{6}$$

B. Formulation of OPF-based model

The main idea of this paper is to study and present different capabilities of PV and EV inverters to provide ancillary services to DSO and improve technical conditions in DN. The objective function is losses minimization and it is formulated in (7).

$$min \sum_{t=1}^{T} \sqrt{P_t^{\mathrm{loss}2} + Q_t^{\mathrm{loss}2}} \tag{7}$$

where P_t^{loss} represents active power losses, while Q_t^{loss} represents reactive power losses in time t.

Balance constraints are formulated as full AC power flows and modeled as bus injection model (BIM) in (8) and (9).

$$P_{i,t} = \sum_{j=i}^{N} |V_{i,t}||V_{j,t}||Y_{ij}| \cos(\delta_{i,t} - \delta_{j,t} - \theta_{ij}) \tag{8}$$

$$Q_{i,t} = \sum_{j=i}^{N} |V_{i,t}||V_{j,t}||Y_{ij}| \sin(\delta_{i,t} - \delta_{j,t} - \theta_{ij}) \tag{9}$$

where:

$P_{i,t}$—active power at bus *i* in time *t*;

$Q_{i,t}$—reactive power at bus *i* in time *t*;

$V_{i,t}$—voltage magnitude at bus *i* in time *t*;

$V_{i,t}$—voltage magnitude at bus *j* in time *t*;

Y_{ij}—*ij*-th element of bus admittance matrix $\mathbf{Y}_{\mathrm{bus}}$;

$\delta_{i,t}$—voltage phase angle at *i*-th bus in time *t*;

$\delta_{i,t}$—voltage phase angle at *j*-th bus in time *t*;

θ_{ij}—phase angle of *ij*-th element of bus admittance matrix $\mathbf{Y}_{\mathrm{bus}}$.

Bus voltage limit (10) represents network operation limits given in grid codes. These limits are defined by $V_i^{\min}$ and $V_i^{\max}$ representing the upper and lower bounds, respectively, and are typically set at $\pm 10\% \mathrm{Un}$ (nominal voltage).

$$V_i^{\min} \leq V_{i,t} \leq V_i^{\max}, \ \forall i \in N, \ \forall t \in T \tag{10}$$

Thermal constraint defined by line current $I_{l,t}$ in time *t* and cable rated current I_l^{nom} is given in 11.

$$I_{l,t} \leq I_l^{nom}, \ \forall l \in L, \ \forall t \in T \tag{11}$$

This relationship between apparent, active and reactive power is defined by the power capability curve (12).

$$S_{pv,t} \leq \sqrt{P_{pv,t}^2 + Q_{pv,t}^2}, \forall pv \in PV, \ \forall t \in T \tag{12}$$

where:

$S_{pv,t}$–PV apparent power in time *t*;

$P_{pv,t}$–PV active power in time *t*;

$Q_{pv,t}$–PV reactive power in time *t*.

PV RPC represents the decision variable bound given in (13). The character of reactive power can be from inductive to capacitive.

$$-P_{pv,t} \cdot \tan\varphi \leq Q_{pv,t} \leq P_{pv,t} \cdot \tan\varphi, \forall\varphi \in [\varphi_{ind}, \varphi_{cap}], \quad \forall pv \in PV, \forall t \in T \tag{13}$$

The PV APC is the second decision variable, its bound is given in (14).

$$P_{pv,t}^{min} \leq P_{pv,t}^{\mathrm{APC}} \leq P_{pv,t}, \ \forall pv \in PV, \forall t \in T \tag{14}$$

where $P_{pv,t}^{\mathrm{APC}}$ is PV APC inverter in time t, $P_{pv,t}$ represents current PV production in time t and $P_{pv,t}^{min}$ minimal PV production in time t.

Lastly, the EV charging bound is expressed in (15).

$$P_{ch,ev,t}^{min} \leq P_{ch,ev,t}^{\mathrm{APC}} \leq P_{ch,ev,t}, \ \forall ev \in EV, \forall t \in T \tag{15}$$

where $P_{ch,ev,t}^{\mathrm{APC}}$ is EV APC inverter in time t, $P_{ch,ev,t}$ represents current EV charging power in time t and $P_{ch,ev,t}^{min}$ minimal EV charging in time t..

III. Co-simulation optimization framework, test network model and case studies description

In this section, the proposed optimization framework is concisely explained. Furthermore, the main information about the test network model is given. Lastly, conducted case studies are presented.

A. Co-simulation optimization framework

Co-simulation optimization interconnects power system simulation tool and computational intelligence (CI) optimization packages with embedded CI optimization algorithms. The communication between the power system simulation tool and the CI optimization package is realized through interfaces. This optimization approach supports using full AC power flows without linearization and relaxation resulting in a more reliable and accurate solution. The proposed optimization framework's primary drawback is its high computational effort requirement. This optimization is called "black-box" optimization in which it focuses exclusively on processing input and producing output, without addressing the intermediate processes.

B. Test network model

The test network model is retrieved from [12]. The transformer substation supplies the observed low-voltage distribution feeder at $10/0.4$ kV. It consists of 83 single-phase end-users with 5-minute resolution different load profiles. Each end-user has an integrated single-phase PV system on its rooftop. Each PV has a defined production profile with a 5-minute resolution and rated power. The observed feeder is well-suited for time-series simulations and provides valuable insights into the dynamic behavior of prosumers. An example of one PV production and load profile is given in Fig. 9 in the Appendix.

C. Case Studies description

The OPF-based model is examined over the following case studies:

- Base Case 1 - all end-users have installed PV system and 15% of end-users own EV with optimization-based charging profile;
- Base Case 2 - all end-users have installed PV system and 15% of end-users own EV with real-life charging profile;
- Case Study 1 - PV RPC when $cos\varphi = 0.80$ and EV APC with optimization-based charging profile and 35% allowable curtailment;
- Case Study 2 - PV APC with 30% allowable curtailment and EV APC with optimization-based charging profile and 35% allowable curtailment;
- Case Study 3 - PV RPC when $cos\varphi = 0.80$ and EV APC with real-life charging profile and 35% allowable curtailment;
- Case Study 4 - PV APC with 30% allowable curtailment and EV APC with a real-life charging profile and 35% allowable curtailment.

The Base Cases include that all end-users have installed PV systems and 15% of them have EVs. The difference is in EV charging profiles- Base Case 1 incorporates an optimization-based charging profile and Base Case 2 includes a real-life charging profile, respectively. The PV RPC operates with $cos\varphi$ of 0.80 inductive and capacitive given by PV inverter manufacturer [13]. The 35% allowable EV charging curtailment is achieved by gradually reducing charging levels while ensuring satisfaction with all network constraints. Another reason is that vehicle owners would not experience dissatisfaction, as the algorithm, considering the R/X network ratio, would aim to fully minimize charging power. The same reason can be applied for 30% of allowable PV curtailment. In the optimization-based EV charging profile, EV charging starts at 00:00 a.m. due to low prices. However, in a real-life model, the EV charging starts at 05:00 p.m. taking into account EV owner habits. The battery capacity of both models is 40 kWh and the charging power is about 7 kW. Both EV charging profiles are presented in Fig. 7 and Fig. 8 in the Appendix.

IV. Results and discussion

This section presents voltage profiles and losses obtained in different case studies. The OPF-based model is codded in *Python* programming language. The *OpenDSS* is used as a power system simulation tool and the *PyGMO* package with CI optimization algorithms is used to solve the optimization problem. The optimization algorithm in this paper is particle swarm optimization (PSO), although any other can be chosen. The optimization procedure is conducted on the one-hour scale. It is essential to emphasize that all figures depicting voltages illustrate their qualitative representation. The voltage profile of each node is presented with a different color.

A. Voltages in Base Cases

Base Case 1) The voltage values at each node are presented in Fig. 1. PVs cause voltage rise in DN. Between 09:00

a.m. and 11:00 p.m., as well as 01:00 p.m. and 02:00 p.m. voltage values exceed the permissible limit of $+10\%\mathrm{Un}$. The highest voltage value is 1.134 p.u. Additionally, EV charging occurs during the period with no PV generation, leading to a voltage drop below the permissible lower limit of $-10\%\mathrm{Un}$. The lowest voltage value is 0.851 p.u. As it can be seen from voltage values, end-users, PVs and EVs are arbitrarily connected to different phases making observed DN highly unbalanced.

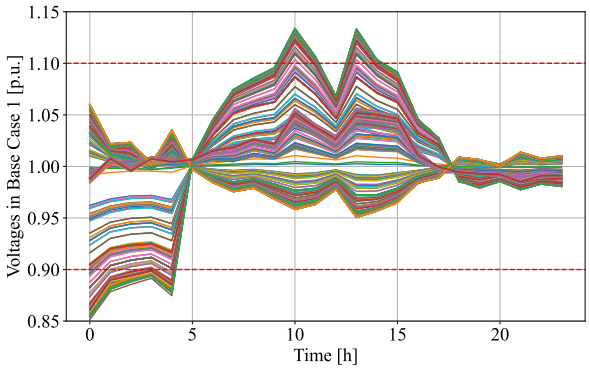

Figure 1. Voltages in Base Case 1

Base Case 2) Fig. 2 shows an indicative representation of voltage values at each node in Base Case 2. As in Base Case 1, there is voltage rise between 09:00 a.m. and 11:00 p.m., as well as 01:00 p.m. and 02:00 p.m. upper the permissible limit of $+10\%\mathrm{Un}$. The highest voltage value is 1.134 p.u. EV charging causes a voltage drop from 05:00 p.m. to 07:00 p.m. The lowest voltage value is 0.864 p.u. which is below the lower voltage limit.

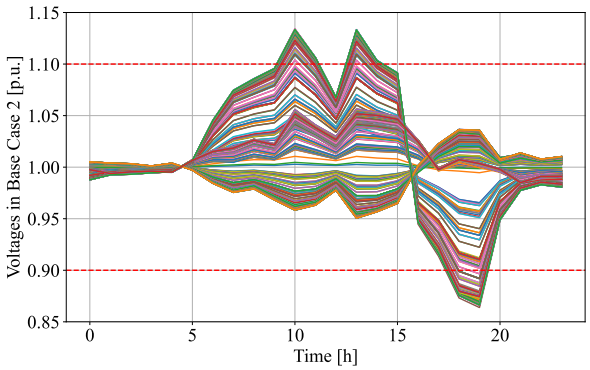

Figure 2. Voltages in Base Case 2

B. Voltages in Case Study 1

Fig. 3 presents voltages at each node in Case Study 1. The highest voltage value is 1.085 p.u., while the lowest is 0.904 p.u. Both control methods ensure that the voltages remain within permissible limits. Additionally, compared to Fig. 1, the reactive power smooths the voltage profile according to the reference value of 1.00 p.u. due to its ability to operate in both inductive and capacitive modes. Furthermore, EV APC ensures that the violated lower voltage limit is within the permitted limits. Reducing the charging power decreases power flow from the network, minimizing voltage drops on the end-user's nodes with EVs.

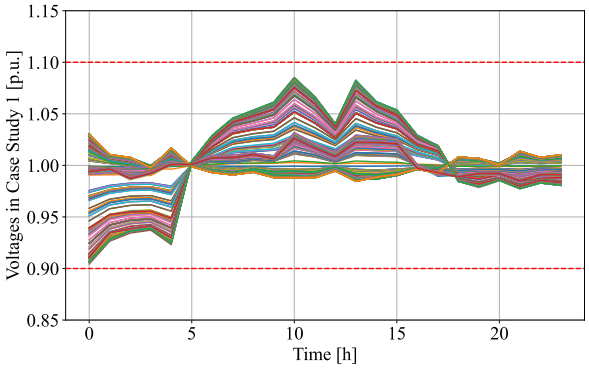

Figure 3. Voltages in Case Study 1

C. Voltages in Case Study 2

Fig. 4 shows voltage values at each node in Case Study 2. This method maintains all voltages within acceptable limits while avoiding unnecessary curtailment of PV production. Without the 30% curtailment limit, imposed by the R/X ratio, the algorithm would minimize production as much as possible significantly reducing end-user satisfaction. The maximum voltage value is 1.089 p.u. and the minimum is 0.904 p.u.

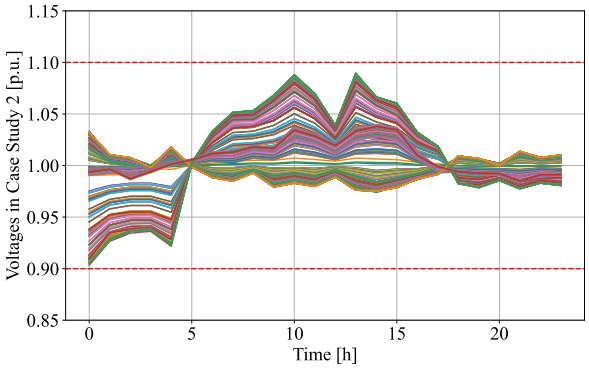

Figure 4. Voltages in Case Study 2

D. Voltages in Case Study 3

The voltage values in Case Study 3 are presented in Fig. 5. A similar conclusion can be made as in Case Study 1. PV RPC and EV APC maintain voltages between limits and make voltage profiles smoother compared to Base Case 2 and Case Study 4. The highest voltage value is 1.086 p.u., while the lowest is 0.911 p.u.

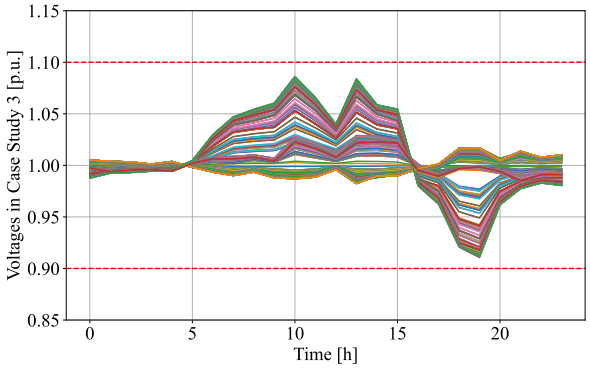

Figure 5. Voltages in Case Study 3

E. Voltages in Case Study 4

Voltage profiles for each node in Case Study 4 are presented in Fig. 6. The combination of PV and EV APC successfully maintains voltage values in allowable limits. The maximum voltage value is 1.091 p.u., while the minimum is 0.911 p.u.

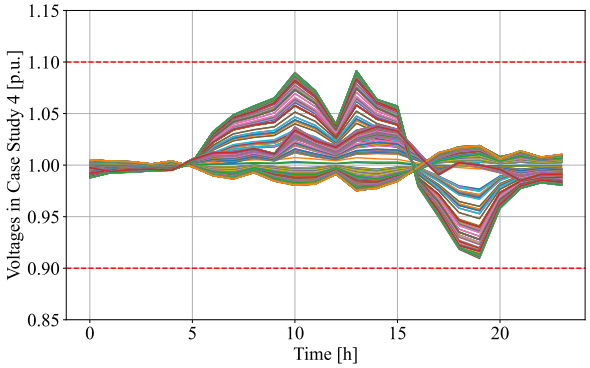

Figure 6. Voltages in Case Study 4

F. Energy losses

Energy losses by active power are presented in Tab. I. The highest losses are in Base Case 1. In this scenario, EV charging and PV production occur temporally independently. When EVs are being charged, power flows from upper network increase. Conversely, PV systems supply power to the observed network, leading to higher power flows toward the upper network. The same explanation can be applied to Base Case 2. EV charging begins when PV production still occurs, resulting in lower losses than in Base Case 1. All proposed control methods successfully reduce energy losses in observed DN. The lowest losses are in Case Study 4.

G. Discussion

Regardless of which control method is applied, they ensure satisfactory voltage conditions in observed DN from a technical point of view. PV RPC can increase and decrease voltages, leading to a lower voltage deviation. On the other hand, due to the R/X ratio, DN is more sensitive to changes in the active power. From an economic point of view, uncoordinated APC violates fairness among PV and EV owners who do not contribute to network issues and may unfairly lose benefits and face penalties. This model considers each PV and EV owner as a potential source of network issues. Therefore, a specific percentage of power is made available for curtailment while ensuring compliance with network constraints. From the DSO point of view, it is necessary to evaluate the profitability of leveraging prosumer capabilities for network operation versus investing in additional equipment. RPC represents a promising solution in the case of minor deviations. However, the question arises as to why the owner would participate in providing ancillary services without receiving compensation.

TABLE I
ENERGY LOSSES IN EACH CASE STUDY.

Case Study	Energy losses [kWh]
Base Case 1	93.75
Base Case 2	80.16
Case Study 1	48.27
Case Study 2	46.06
Case Study 3	42.39
Case Study 4	36.51

Regarding to Base Cases losses are reduced with all control methods. Compared to Base Case 1 losses are decreased by 47.81% in Case Study 1 and 50.87% in Case Study 2, respectively. Furthermore, losses are reduced by 47.12% in Case Study 3 and 54.45% in Case Study 4 in regard to Base Case 2.

V. CONCLUSION

This paper proposes an OPF-based model for improving technical conditions in DN with PV and EV. The paper uses the capabilities of PV and EV inverters as control variables. Four case studies are presented to test the effectiveness of the proposed model. The model is evaluated over DN modelled according to the real-life model. According to the obtained results, the proposed model shows potential for providing ancillary services and participation in DN operation optimization.

The future research includes an economic analysis of the proposed from both DSO and prosumer points of view.

ACKNOWLEDGMENT

The work of doctoral student Marina Dubravac has been fully supported/supported in part by the "Young researchers' career development project – training of doctoral students"(DOK-2021-02-1257) of the Croatian Science Foundation. This work was founded by Croatian Science Foundation under the project "Prosumer-rich distribution power network" (project number: UIP-2020-02-5796) and the European Union's Horizon Europe Framework Programme: HORIZONWIDERA-2023-ACCESS-04, Pathways to Synergies—Coordination and Support Actions—under the project name SynGRID—Creating synergies in Widening countries on the topic of low-voltage grid management (grant number 101160145).

REFERENCES

[1] V. Kumar Tatikayala and S. Dixit, "Multi-stage voltage control in high photovoltaic based distributed generation penetrated distribution system considering smart inverter reactive power capability," *Ain Shams Engineering Journal*, p. 102265, 2023. [Online]. Available: https://doi.org/10.1016/j.asej.2023.102265

[2] M. Dubravac, K. Fekete, D. Topić, and M. Barukčić, "Voltage Optimization in PV-Rich Distribution Networks—A Review," *Applied Sciences (Switzerland)*, vol. 12, no. 23, 2022.

[3] D. Gebbran, S. Mhanna, Y. Ma, A. C. Chapman, and G. Verbič, "Fair coordination of distributed energy resources with Volt-Var control and PV curtailment," *Applied Energy*, vol. 286, no. January, p. 116546, 2021. [Online]. Available: https://doi.org/10.1016/j.apenergy.2021.116546

[4] A. Demirci, S. M. Tercan, E. E. Ahmed, U. Cali, and I. Nakir, "A novel electric vehicle charging management with dynamic active power curtailment framework for PV-rich prosumers," *IEEE Access*, vol. 12, no. August, pp. 120 239–120 249, 2024.

[5] X. Li, C. Yip, Z. Y. Dong, C. Zhang, and B. Wang, "Hierarchical control on EV charging stations with ancillary service functions for PV hosting capacity maximization in unbalanced distribution networks," *International Journal of Electrical Power and Energy Systems*, vol. 160, no. January 2023, p. 110097, 2024. [Online]. Available: https://doi.org/10.1016/j.ijepes.2024.110097

[6] S. Toghranegar, A. Rabiee, and S. M. Mohseni-Bonab, "Increasing Unbalanced Distribution Network's Hosting Capacity for Distributed Energy Resources by Voltage Regulators," *IEEE Access*, vol. 11, no. March, pp. 22 664–22 679, 2023.

[7] N. Mizuta, Y. Susuki, Y. Ota, and A. Ishigame, "Synthesis of Spatial Charging/Discharging Patterns of In-Vehicle Batteries for Provision of Ancillary Service and Mitigation of Voltage Impact," *IEEE Systems Journal*, vol. 13, no. 3, pp. 3443–3453, 2019.

[8] A. F. Soofi and S. D. Manshadi, "Unleashing grid services potential of electric vehicles for the Volt/Var optimization problem," *IEEE Transactions on Vehicular Technology*, vol. 72, no. 11, pp. 14 115–14 126, 2023.

[9] R. Kljajić, P. Marić, N. Mišljenović, and M. Dubravac, "An Optimized Strategy for the Integration of Photovoltaic Systems and Electric Vehicles into the Real Distribution Grid," *Energies*, vol. 17, no. 22, 2024.

[10] M. Dubravac, D. Topić, K. Fekete, Z. Šimić, R. Prenc, and M. Rojnić, "Active power curtailment and reactive power control in pv-rich low-voltage distribution network," in *2024 20th International Conference on the European Energy Market (EEM)*, 2024, pp. 1–6.

[11] "CROATIAN POWER EXCHANGE." [Online]. Available: https://www.cropex.hr/en/

[12] "Electricity North West," 2015. [Online]. Available: https://www.enwl.co.uk/future-energy/innovation/smaller-projects/low-carbon-networks-fund/low-voltage-network-solutions/

[13] "Growatt." [Online]. Available: https://en.growatt.com/

APPENDIX

EV charging profile obtained from measurements is presented in Fig. 7. The measurement was carried out on 10-minute values, which were scaled to hourly values.

EV charging profile obtained from optimization is presented in Fig. 8.

An example of PV production and load profile is given in Fig. 9.

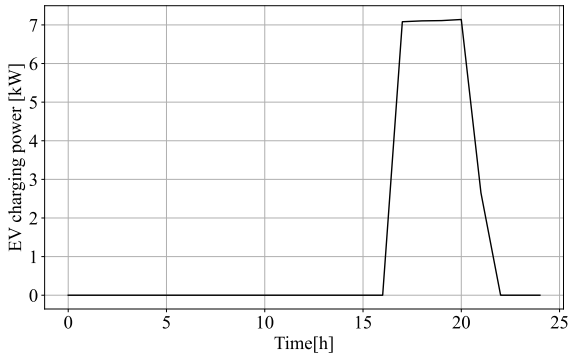

Figure 7. EV charging profile obtained from measurements

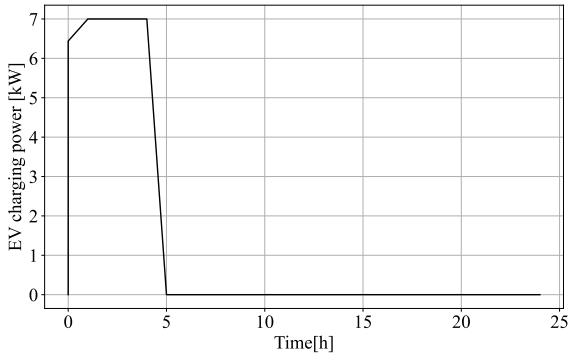

Figure 8. EV charging profile obtained from optimization

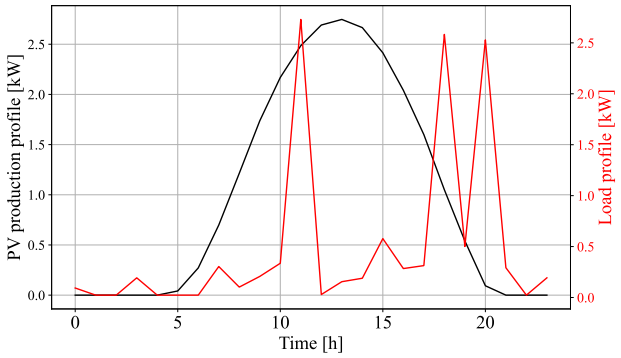

Figure 9. PV production and load profile